To be submitted to
Nuclear Phys.

ISTITUTO NAZIONALE DI FISICA NUCLEARE
Laboratori Nazionali di Frascati

LNF-80/46(P)
27 Agosto 1980

M. Consoli and M. Greco: RADIATIVE CORRECTIONS TO VERY HIGH ENERGY ELECTRON-PROTON SCATTERING.

Servizio Documentazione
dei Laboratori Nazionali di Frascati

INFN-Laboratori Nazionali di Frascati
Servizio Documentazione

LNF-80/46(P)
27 Agosto 1980

M. Consoli(*) and M. Greco: RADIATIVE CORRECTIONS TO VERY HIGH ENERGY ELECTRON-PROTON SCATTERING.

ABSTRACT

A "leading log" analysis of radiative corrections to inclusive e-p scattering at HERA energies is presented. Neutral current weak interactions are considered at the level of Born cross section as well as of the modifications of vertex and vacuum polarization parts. The leading log approximation has been also improved in the single hard and multiple soft photon emission by appropriate kinematical considerations. Some numerical results are presented for polarized electron and positron beams.

1. - INTRODUCTION

Lepton-hadron collisions have been a copious source of information about both charged and neutral current weak interactions, as well as about the nature of the elementary constituents of hadrons. A very high energy electron-proton storage ring is now under study[1] (HERA). The large momenta available will unable us to probe for the hadron as well as lepton substructure on a much smaller distance scale than previously possible. In particular the momentum tranfer Q will be of the same order of the rest masses of the $W^{\pm}$ and Z_o, and the weak and electromagnetic interactions of comparable magnitude.

Obviously, no reliable information can be extracted from such high energy experiments unless the problem of radiative corrections is fairly well understood. In the past, radiative corrections have been applied[2] to the data on elastic and deep inelastic electron scattering by taking into account bremsstrahlung and virtual effects in the electron legs as well as photon propagator corrections and disregarding weak interactions effects. Recently, an improved leading logarithmic approximation has been discussed[3] in the computation of the radiative corrections to high-energy neutrino scattering. By correctly taking into account the kinematical limits in the

(*) Istituto di Fisica Teorica dell'Università, Catania and INFN, Sezione di Catania.

photon phase-space, the accuracy of the usual leading log approximation has been shown to improve near the edges of the x,y kinematical range, where x and y are the usual scaling variables.

In this paper we present an analysis of the most important radiative effects in electron nucleon collisions at very high energies. Due to the large Q^2 values experimentally accessible and the smallness of the electron mass we will restrict to the leading corrections $\propto \alpha \ln Q^2/m^2$. Furthermore, following ref. (3), this leading-log approximations has been improved both in the single hard and multiple soft photon emission. The role played by weak interactions has been considered both at the level of the Born cross sections and of the modification of the vertex and vacuum polarization parts.

Photon emission from the hadron legs has been disregarded for two main reasons. First, the usual measurements of the hadronic structure functions are totally inclusive, irrespective of whether photons do or do not accompany the final hadronic state. Second, due to the cancellations of the quark mass singularities in the observable cross sections[4], the resulting expressions, of order α , only depend on various ratios of the kinematical variables and can be safely neglected in our approximation.

Our results are therefore valid up to terms of order α , and quite accurate everywhere except at the very edges of the x,y phase space, as discussed in more detail below.

The paper is organized as follows. In section 2. we give the expressions of the Born cross sections as well as the parametization of the quark distributions used in the numerical applications. In section 3. finite first order virtual corrections are studied. Real photon effects, both soft and hard, are discussed in section 4., together with the limits of validity of our expressions. Some numerical results and our conclusions are finally presentd in section 5. for $e^{\pm}_{L,R}$-proton scattering.

The following notations are used: m=electron mass, μ= muon mass, M_o= neutral vector boson mass, $s_w = \sin\theta_w$ (θ_w being the weak mixing angle[5]), $c_w = \cos\theta_w$ and g = SU(2) coupling constant. The incoming electron four-momentum is denoted as k, p is the incoming proton and k' is the outgoing electron. Finally $s = -(p+k)^2$, $Q^2=(k-k')^2$, $\nu=p.Q$, $x=Q^2/2\nu$ and $y=\nu/\nu_{max}$.

2. - BORN TERMS

The Born terms are given by the two diagrams of Fig. 1, for which the scattering amplitude reads

FIG. 1 - Born diagrams for the neutral current process $e+p \rightarrow e^- + X$.

$$M_A = g^2\, l^{\gamma}_{\mu}\ \frac{1}{Q^2}\ \langle n/J^{\gamma}_{\mu}/p\rangle, \qquad M_B = g^2\, l^{w}_{\mu}\ \frac{1}{Q^2+M_o^2}\ \langle n/J^{w}_{\mu}/p\rangle, \tag{2.1}$$

where

$$l^{\gamma}_{\mu} = \bar{e}'\gamma_{\mu}\ (a^{\gamma} + b^{\gamma}\ \gamma_5)e, \qquad l^{w}_{\mu} = \bar{e}'\ \gamma_{\mu}\ (a^{w} + b^{w}\ \gamma_5)e, \tag{2.2}$$

and

$$a^{\gamma} = -\ s_w, \qquad b^{\gamma} = 0,$$
$$a^{w} = \frac{4s_w^2 - 1}{4c_w}, \qquad b^{w} = -\frac{1}{4c_w}. \tag{2.3}$$

The double differential inclusive cross sections for $e^{+}_{L,R}$ are given by

$$\frac{d\sigma^{Born}(e^{-}_{L,R})}{dx\,dy} = \frac{g^4}{\pi}\ \frac{1}{s\,x^2\,y^2}\ \Big\{\ g^{\gamma\,2}_{L,R}\ F^{\gamma\gamma}(x,y) + 2Z\ g^{w}_{L,R}\ g^{\gamma}_{L,R}\ F^{\gamma w}_{-,+}(x,y) + Z^2\ g^{w\,2}_{L,R}\ F^{ww}_{-,+}(x,y)\ \Big\},$$
$$\frac{d\sigma^{Born}(e^{+}_{L,R})}{dx\,dy} = \frac{g^4}{\pi}\ \frac{1}{s\,x^2\,y^2}\ \Big\{\ g^{\gamma\,2}_{R,L}\ F^{\gamma\gamma}(x,y) + 2\,Z\ g^{w}_{R,L}\ g^{\gamma}_{R,L}\ F^{\gamma\,w}_{-,+} + Z^2\ g^{w\,2}_{R,L}\ F^{ww}_{-,+}(x,y)\ \Big\}, \tag{2.4}$$

where ($i = \gamma, w$)

$$g^{(i)}_{L,R} = \frac{1}{2}\,(a^{(i)} \pm b^{(i)}), \tag{2.5}$$

$$Z = \frac{Q^2}{Q^2 + M_o^2}, \tag{2.6}$$

$$F^{\gamma\gamma}(x,y) = x\,y^2\,F_1^{\gamma\gamma}(x) + (1-\cdots)\,F_2^{\gamma\gamma}(x), \tag{2.7}$$

$$F^{ij}_{-,+}(x,y) = x\,y^2\,F_1^{ij}(x) + (1-y)\,F_2^{ij}(x) \mp x\,y\,(1-\frac{y}{2})\,F_3^{ij}(x), \tag{2.8}$$

and the various $F_{1,2,3}$ are the usual structure functions which, for simplicity have been assumed to scale.

In terms of the quark-parton distributions and their axial-vector couplings to the electro-weak currents we have

$$F_2^{ij}(x) = \sum_q x \left[q(x) + \bar{q}(x)\right] \left[a^i a^j + b^i b^j\right], \tag{2.9}$$

$$x F_3^{ij}(x) = - \sum_q x \left[q(x) - \bar{q}(x)\right] \left[a^i b^j + b^i a^j\right], \tag{2.10}$$

and we have assumed the Callan-Gross relation

$$F_2^{ij}(x) = 2 x F_1^{ij}(x). \tag{2.11}$$

For the up-quarks (u,c) we have

$$a^\gamma = \frac{2}{3} s_w, \qquad b^\gamma = 0,$$

$$a^W = \left(1 - \frac{8}{3} s_w^2\right) \frac{1}{4c_w}, \quad b^W = \frac{1}{4c_w}, \tag{2.12}$$

whereas for the down quarks (d,s)

$$a^\gamma = -\frac{1}{3} s_w, \qquad b^\gamma = 0,$$

$$a^W = \left(\frac{4}{3} s_w^2 - 1\right) \frac{1}{4c_w}, \qquad b^W = -\frac{1}{4c_w}. \tag{2.13}$$

In our numerical applications we shall use the following distributions for the valence quarks[6]

$$x \left[u_v(x) + d_v(x)\right] = \frac{3}{B(\alpha_3, \alpha_4 + 1)} x^{\alpha_3} (1-x)^{\alpha_4},$$

$$x d_v(x) = \frac{1}{B(\alpha_1, \alpha_2 + 1)} x^{\alpha_1} (1-x)^{\alpha_2}, \tag{2.14}$$

with $\alpha_1 = 0.89$, $\alpha_2 = 3.78$, $\alpha_3 = 0.65$ and $\alpha_4 = 3$.

For the sea contributions we have used[6]

$$x \bar{u}(x) = x \bar{d}(x) = 0.15 (1 - x)^7,$$

$$x s(x) = 0.06 (1 - x)^7, \tag{2.15}$$

$$x c(x) = 0.02 (1 - x)^7.$$

Scaling violations can, of course, be taken into account by appropriate use of Q^2-dependent quark distributions.

The various Born cross section given in eqs. (2.4) normalized to the pure one photon exchange, are shown in Fig. (2) for $s = 100.000$ GeV^2, whereas the lowest order left-right asymmetry for electrons is presented in Fig. 3.

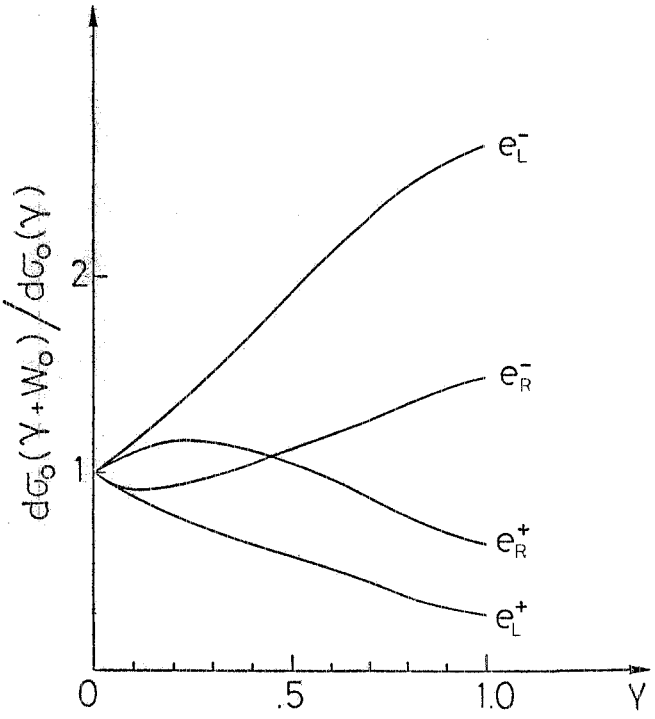

FIG. 2 - Born cross sections for different helicity lepton beams s=100.000 Gev^2 and s_w^2 =0.24.

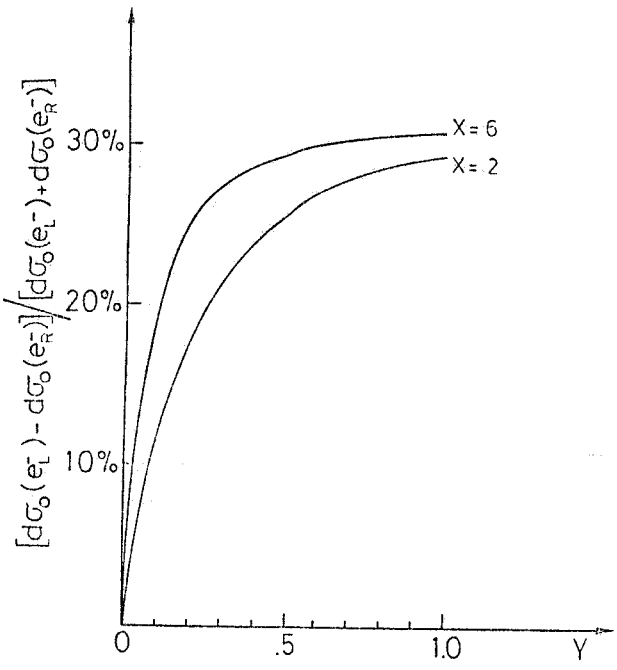

FIG. 3 - Lowest order left-right asymmetry for electrons for s=100.000 GeV^2 and s_w^2=0.24.

3. - VIRTUAL CORRECTIONS

As stated in the introduction, we shall restrict to the leading corrections $\propto \alpha \ln Q^2/m^2$. Our results are therefore approximate up to terms of order α/π. The vertex and vacuum polarization parts modify the bare electromagnetic and weak lepton current as shown in Fig. 4.

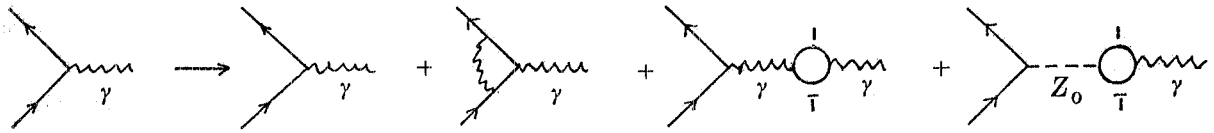

FIG. 4 - Vertex and vacuum polarization modifications to the bare electromagnetic lepton current.

This amounts to the replacements in eq. (2.3):

$$a^\gamma \to A^\gamma = a^\gamma \left\{ 1 + \frac{g^2}{16\pi^2} \left[3 s_w^2 \ln \frac{Q^2}{m^2} + \right.\right.$$

$$\left.\left. + \frac{4}{3} \left(s_w^2 + \frac{(4 s_w^2 - 1)^2}{16 c_w^2} \right) Z \sum_l \ln \frac{Q^2}{m_l^2} \right] \right\}, \qquad (3.1)$$

$$b^{\gamma} \rightarrow B^{\gamma} = -\frac{g^2}{16\pi^2}\, s_w \frac{(1-4s_w^2)}{16c_w^2}\, Z\, \frac{4}{3} \sum_l \ln \frac{Q^2}{m_l^2} \quad . \tag{3.1}$$

and the sum in the r.h.s. is over different lepton families. Analogously for the weak current we have (see Fig. 5).

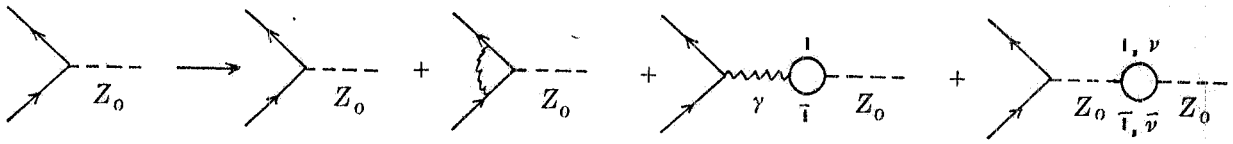

FIG. 5 - Vertex and vacuum polarization modifications to the bare weak lepton current.

$$a^W \rightarrow A^W = a^W \left\{ 1 + \frac{g^2}{16\pi^2} \left[3 s_w^2 \ln \frac{Q^2}{m^2} + \frac{4}{3}\left(s_w^2 + \frac{(4s_w^2-1)^2+3}{16 c_w^2}\right) Z \sum_l \ln \frac{Q^2}{m_l^2} \right] \right\},$$

$$b^W \rightarrow B^W = b^W \left\{ 1 + \frac{g^2}{16\pi^2} \left[3 s_w^2 \ln \frac{Q^2}{m^2} + \frac{4}{3} \frac{(4s_w^2-1)^2+3}{16 c_w^2} Z \sum_l \ln \frac{Q^2}{m_l^2} \right] \right\}. \tag{3.2}$$

The above expressions have been obtained by fixing the finite parts of the ultraviolet divergent diagrams through the renormalization prescription given in ref. (7). For the numerical evaluations only electron and muon loops have been taken into account.

The hadronic contributions to the various self-energy parts can be, in principle, evaluated using dispersion relations techniques. However, whereas for the photon self-energy one can directly use the experimental data from $e^+ e^-$ annihilations, for the mixing terms and the neutral vector boson self-energy the corresponding contributions would require a careful analysis of the different isospin and parity components of the final hadronic states. In the present analysis those hadronic contributions have not been considered .

The infrared divergent part coming from vertex corrections will be discussed in the next section together with the multiple soft photon bremsstrahlung.

Finally let us briefly comment on the contribution from two (and more) photon exchanges between the electron and the parton's lines. It has been suggested[8] that the n-photon exchange behaves, to leading order, as $(\ln^2 Q^2)^{n-1}$, leading to sizeable corrections to deep inelastic e-N scattering at large Q^2. Although the result[9] is formally correct at fixed t, in the actual cases of experimental interest, the scale mass in the logarithm is always given by some large kinematical variable, e.g. s,t, u, ... , such that the final correction is never competitive with $\ln Q^2/m^2$.This has been explicitly shown in the case of e-μ scattering[10]. A quark mass scale in $(\ln^2 Q^2)^{n-1}$ is also unreasonable, because of the cancellation of the quark mass singularities in the observable cross sections[4]. Therefore we will also disregard, for constistency, these finite corrections of order α.

4. - REAL PHOTON CORRECTIONS

Bremsstrahlung effects in deep inelastic scattering have been extensively discussed in the literature. In particular it has been shown[2] that the so called peaking approximation works quite well as long as the x and y kinematical bounds are not approached too much. The accuracy of this leading log approximation has been further improved[3] in this restricted region of phase space by taking correctly into account the kinematical limits of the emitted photon.

In the following, we will consider multiple soft photon effects by keeping trace in the hadronic vertex of the emitted radiation, as well as hard emission with the correct photon kinematics. We expect therefore that our expressions will be enough accurate also when x and y approach 0 and 1. A more detailed discussion on this point is given below.

As well known, multiple soft bremsstrahlung amounts to take into account processes as in Fig. 6, where the total amount of the radiated energy is smaller than some quantity $\Delta\omega$, which is generally related to the experimental resolution.

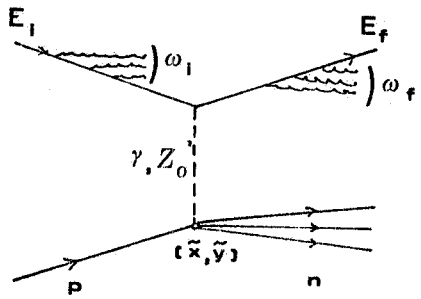

FIG. 6 - Multiple soft bremsstrahlung diagrams. The modified hadronic scaling variables $\tilde{x}$ and $\tilde{y}$ are defined in the text.

Defining the auxiliary variables z_1 and z_2 as

$$z_1 E_i = E_i - \omega_i , \qquad \frac{E_f}{z_2} = E_f + \omega_f , \tag{4.1}$$

the hadronic scaling variables x and y are modified, in the approximation of photon collinear to either the incident or the scattering electron, as

$$x \to \tilde{x} = \frac{z_1 x y}{z_1 z_2 + y - 1} , \qquad y \to \tilde{y} = \frac{z_1 z_2 + y - 1}{z_1 z_2} . \tag{4.2}$$

Of course the range of z_1 and z_2 values is restricted by the conditions $0 \leq \tilde{x}, \tilde{y} \leq 1$ and $\omega_i + \omega_f \leq \Delta\omega$. Defining $\Delta \equiv \Delta\omega/E_i$, the first condition leads to

$$\Delta \leq \frac{y(1 - x - y + xy)}{1 - y + xy} \equiv \Delta_M , \tag{4.3}$$

whereas the latter gives

$$z_{2min} \equiv \frac{1-y}{1-y+\Delta} \leq z_2 \leq 1, \qquad z_{1min} \equiv \frac{1-y}{z_2} + y - \Delta \leq z_1 \leq 1. \tag{4.4}$$

The above condition (4.3) is quite stringent in some region near the kinematical bounds, as explicitly shown in Table I.

TABLE I

The quantity Δ_M defined in (4.3) for different values of x and y.

x \ y	0.1	0.3	0.5	0.7	0.9
0.1	0.089	0.259	0.409	0.510	0.426
0.3	0.067	0.185	0.269	0.288	0.170
0.5	0.047	0.123	0.166	0.161	0.081
0.7	0.027	0.069	0.088	0.079	0.036
0.9	0.009	0.021	0.026	0.022	0.0098

Then the usual exponentiation of multiple soft photon leads to

$$\frac{d\sigma^{soft}}{dx\,dy} = \beta^2 \int_{z_{2min}}^{1} \frac{dz_2}{z_2} \left[f(z_2)\right]^{1-\beta} \int_{z_{1min}}^{1} dz_1 \left[f(z_1)\right]^{1-\beta} F(z_1,z_2), \tag{4.5}$$

where

$$f(z) = \frac{1}{1-z}\left(\frac{1+z^2}{2}\right), \tag{4.6}$$

$$F(z_1,z_2) = \frac{y}{z_1 z_2 + y - 1} \left[\frac{d\sigma^{Born}(x,y)}{dx\,dy}\right]_{\substack{x=\tilde{x} \\ y=\tilde{y}}} \tag{4.7}$$

and

$$\beta = \frac{\alpha}{\pi} \ln\frac{Q^2}{m^2}\,. \tag{4.8}$$

In the approximation $z_1, z_2 \sim 1$, $\tilde{x}$ and $\tilde{y}$ approach x and y respectively and eq. (4.5) gives the usual result

$$\frac{d\sigma^{soft}}{dx\,dy} \sim \frac{d\sigma^{Born}}{dx\,dy}\,\Delta^{2\beta}\,. \tag{4.9}$$

The hard photon contributions are shown in Fig. 7,

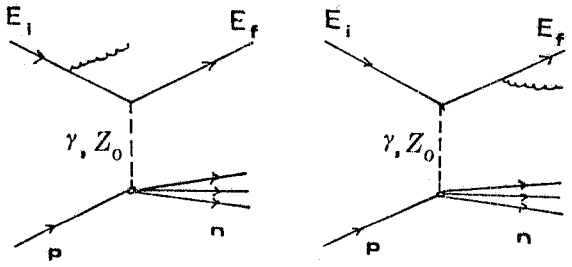

FIG. 7 - Hard bremsstrahlung diagrams.

and are given by

$$\frac{d\sigma_1^{hard}}{dx\,dy} = \beta_i \int_{u_{1min}}^{u_{1max}} du_1\, f(u_1)\, F(u_1,1)$$

$$\frac{d\sigma_2^{hard}}{dx\,dy} = \beta_f \int_{u_{2min}}^{u_{2min}} \frac{du_2}{u_2}\, f(u_2)\, F(1,u_2), \tag{4.10}$$

where $f(u_{1,2})$ and $F(u_1, u_2)$ are defined in eqs. (4.6) and (4.7) and

$$u_{1min} = \frac{1-y}{1-xy}\ , \qquad u_{1max} = 1 - \Delta\ ,$$

$$u_{2min} = 1 - y + xy\ , \qquad u_{2max} = \frac{1-y}{1-y+\Delta}\ . \tag{4.11}$$

Furthermore the bound $\Delta \lesssim \Delta_M$ (eq. (4.3)) ensures that $u_{1min} < u_{1max}$ and $u_{2min} < u_{2max}$. Finally β_i and β_f are the logarithmic factors

$$\beta_i = \frac{\alpha}{\pi} \ln s/m^2, \qquad \beta_f = \frac{\alpha}{\pi} \ln \frac{s(1-y+xy)^2}{m^2} \tag{4.12}$$

which, in place of β (eq. (4.8)), improve[3] the accuracy of the leading logarithmic approximation near the kinematical bounds, limiting the relevance of constant neglected terms to simple logarithmics of x,y, 1-x and 1-y.

By comparing the expressions (4.5) and (4.10) for soft and hard bremsstrahlung it is clear that Δ cannot be chosen neather too small, for the validity of the single hard photon approximation, nor too large, for the use of the exponentiated form (4.5). A natural choice is too use the kinematical bound (4.3) when $\Delta_M \lesssim 0.1$ and a fixed values $\Delta \sim 0.1$ when Δ_M becomes large, particularly in the region of small x and large y (see Table I).

5. - NUMERICAL RESULTS

From the previous discussion we can put the observable double differential cross section in the form

$$\frac{d\sigma^{obs}}{dx\,dy} = \frac{d\sigma^{Born}}{dx\,dy} \left[1 + \delta\ (x,y) \right], \tag{5.1}$$

where δ (x,y) includes all possible corrections and is reported in Figs. 8 and 9 in the case of left-handed electrons and right-handed positrons respectively, for s=100.000 GeV^2 and s_w^2=0.24. The main contribution is due to pure QED corrections (both virtual and real) so that there are no substantial differences between the various types of particles. For this reason we have not explicitly reported the radiative corrections relative to right-handed electrons and left-handed positrons. Therefore the ratios between the various lowest order cross sections and all

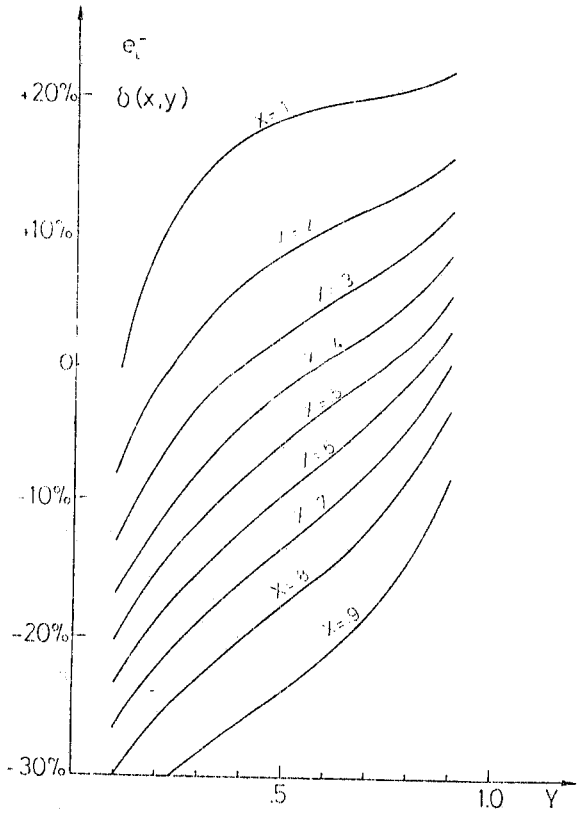

FIG. 8 - Total correction to the Born cross section for left-handed electrons, for s=100.000 GeV^2 and s_w^2 = 0.24.

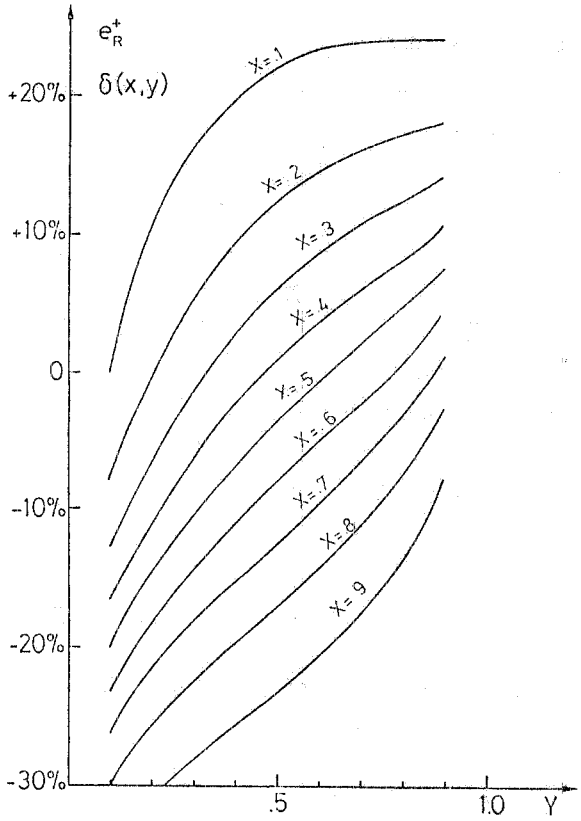

FIG. 9 - Total correction to the Born cross section for right-handed positrons, for s= =100.000 GeV^2 and s_w^2 =0.24.

the macroscopic features due to electro-weak interference are preserved.

A few words are of order to discuss the dependence of our results on Δ. Since Δ is not a physical quantity determined experimentally, the overall result should be, in principle, Δ-independent. However, this is not the actual case because the soft photon corrections are treated in exponentiated form, whereas the hard photon part is taken to first order. A rough estimate of this effect is obtained by replacing $2\beta \ln \Delta$ with $(\Delta^{2\beta} - 1)$ for the soft correction. For Δ =0.1 and a tipical value $\beta \sim 0.058$ (see eq. (4.8)) this changes the soft photon correction from -27% to -24%, whereas for Δ =0.01 the variation is from -53% to -41%. Besides, for Δ very small, the hard photon approximation gets poor.

On the other hand one cannot use the same value of Δ in the entire kinematical range because the parton distributions are very sensitive to small variations in x and therefore new scaled variables x and y have to be used. This in turn puts physical limitations on Δ, as explicity discussed in the previous section.

From the above considerations it follows that our results are quite reliable to a level of $\lesssim$ 10% of the soft correction, particularly not very near the (x,y) kinematical bounds (see Table I) where non-leading terms, neglected in our approximation, make anyhow our results not very accurate.

To conclude, we have presented improved leading log radiative corrections to deep inelastic e-p scattering at very high energies, including the main effects due to neutral current weak interactions.

REFERENCES

(1) Study on the proton-electron storage ring project HERA, ECFA 80/42 and DESY HERA 80/01, March (1980).
(2) For a review, see L.W. Mo and Y.S. Tsai, Rev. Mod. Phys. 41, 205 (1969).
(3) A. De Rujula, R. Petronzio and A. Savoy-Navarro, Nuclear Phys. B154, 394 (1979).
(4) T. Kinoshita, J. Math. Phys. 3, 650 (1962); T.D. Lee and M. Nanenberg, Phys. Rev. 133, 1549 (1964).
(5) S. Weinberg, Phys. Rev. Letters 19, 1264 (1967); A. Salam, Proc. 8th Nobel Symp., Stockholm 1968, ed. N. Svartholm (Almquist and Wiksells).
(6) F. Martin, contribution to the "Proc. of the Study of an e-p Facility for Europe", U. Amaldi Editor, DESY, Hamburg, (April 1979).
(7) F. Antonelli, M. Consoli, G. Corbò and O. Pellegrino, "The masses of the intermediate vector bosons", submitted to Nuclear Phys. B.
(8) J. Bartels, Nuclear Phys. B82, 172 (1974).
(9) V.G. Gorshkov, V.N. Gribov, L.N. Lipatov and G.V. Frolov, Yad. Phys. (USSR) 6, 129 and 361 (1967).
(10) K.E. Eriksson, Nuovo Cimento 19, 1029 (1961).